



# Ultrasonic heating and temperature measurement in microfluidic channels

Goksen Yaralioglu\*

Ginzton Laboratory, Stanford University, Stanford, CA 94305, United States

## ARTICLE INFO

### Article history:

Received 23 December 2010  
Received in revised form 9 May 2011  
Accepted 11 May 2011  
Available online 2 June 2011

### Keywords:

Ultrasonic  
Microfluidics  
Temperature measurement

## ABSTRACT

Microfluidic devices integrated with ultrasonic transducers were developed. Piezoelectric thin film based transducers and capacitive micromachined ultrasonic transducers (CMUTs) were integrated with microchannels. While piezoelectric transducers operated in the vicinity of 400 MHz, the operation frequency of the CMUTs was approximately 50 MHz. Ultrasound generated by the transducers was used for both heating the liquid and sensing the temperature of the liquid inside the channel. The temperature measurement method depends on the time of flight monitoring of the acoustic reflections inside the channel. The method was applied to channels with different heights from 200  $\mu\text{m}$  to 500  $\mu\text{m}$ . The accuracy of the method was found to be 0.1  $^{\circ}\text{C}$ . The measurement bandwidth could be as high as 1 MHz.

© 2011 Elsevier B.V. All rights reserved.

## 1. Introduction

Miniaturization of bio-fluidic systems enables analysis of biological specimens in nano-liter to micro-liter volumes [1–4]. However, bulky instrumentation, such as lasers, CCD cameras, pumps or hot plates, is used for sensing and actuation in such small volumes. This therefore limits the portability of microfluidic devices. Ultrasound generated by integrated transducers with fluidic channels offers a possible solution to this problem. Acoustic waves that are generated by the transducers comparable to the microchannels in size can be used for both fluid actuation and sensing. In the previous research, ultrasound was applied successfully for microfluidic mixing [5]. In this study, we used ultrasonic waves to monitor the temperature of the fluid in the microfluidic channels. Ultrasound was generated by means of integrated transducers into the channels. Moreover, continuous wave excitation of these transducers could heat the fluids inside the channel.

One particular parameter of interest in microfluidic analysis is the fluid temperature. Many biochemical interactions such as amplification of DNA by polymerase chain reaction (PCR) require precise control of temperature [6,7]. Different methods have so far been reported for temperature monitoring. Ross et al. used fluorescence microscopy and acquired images of the fluorescence intensity of a dilute fluorophore using a CCD camera [8]. This technique achieves very high spatial accuracy ( $\sim 1 \mu\text{m}$ ) but its bandwidth is limited by the refresh rate of the CCD. It also requires an imaging optics and a camera, which makes the method unsuitable for portable devices. In addition, fluorescent chemicals may affect

the chemical reaction under investigation. In a similar approach, thermochromic liquid crystals (TLCs) were used [9,10]. TLC suspension changes color with temperature fluctuations. By measuring the reflected light spectrum from the TLC suspension using a spectrometer, one can determine the temperature in a microfluidic channel. In another study, Lao et al. developed a technique where the resistivity of metal electrodes was used to measure temperature in a small chamber [11]. Their system is relatively large and the measurement method is sensitive to the temperature of the substrate and the surrounding material. This method measures the temperature of the electrode, which may be different from the rest of the chamber. It measures the average resistivity of a long resistor over a relatively large volume of liquid as well. Laser-based temperature measurement systems have also been developed. Fan and Longtin used a laser beam to measure the reflectivity of the interface between the substrate and the fluid [12]. The reflectivity depends on the refraction index of the fluid, which varies with the temperature. This technique can achieve high temporal and spatial resolution. But it requires a laser and a focusing optics. In another approach, one wall of the microfluidic channel is made with embedded thermoindicators [13]. This method again requires a CCD camera and it is not very accurate. The other methods for temperature measurement include interferometry [14], NMR thermometry [15], Raman spectroscopy [16,17] and interferometric back scatter detection [18]. These methods either require very expensive instrumentation or are not very sensitive. On the heating side, the most common methods are to use a Peltier device [19] or a resistor [11,20]. These two methods enable relatively easy heating methods, but it is difficult to control where the heat is applied because these devices usually heat up one wall of the channel where they are embedded or attached. This may potentially be a problem for very small form factor devices. Joule heating was also

\* Corresponding author.

E-mail address: [goksenin@gmail.com](mailto:goksenin@gmail.com)

proposed for liquid heating [21]. This method is only applicable for conductive liquids.

In this article, we describe an ultrasound based method for accurate determination of temperature in a microfluidic channel. This method uses the time of flight measurement of ultrasonic reflections from the microfluidic channel. The sound velocity in the fluid determines the time of flight of the acoustic reflections inside the liquid. Sound velocity varies as the fluid temperature changes. Hence, by monitoring the velocity, one can determine the liquid temperature. Inherently, this method is only sensitive to the temperature of the liquid and independent of the temperature of the substrate or the channel material. Since it uses very low energy ultrasonic pulses, it is completely non-invasive. Moreover, potentially this method can integrate all the measurement electronics in a small footprint and there is no alignment requirement as in the case of laser-based methods. In addition to the temperature sensing, the transducers can also be used to heat the liquid. When the transducers are used to generate a continuous acoustic field inside the liquid, the absorption of the ultrasound increases the liquid temperature. By using this method, one can get a very well controlled liquid heating without heating the channel walls directly other than heat conduction.

Ultrasound has been used in detecting temperature, flow or particles in macrochannels for a long time [22–24]. Ultrasonic measurement techniques use time of flight, phase or amplitude measurements of the reflected acoustic waves from the channel walls or from the particles inside the channels. Usually one or more transducers are employed for the measurements. The temperature is usually monitored by measuring the time of flight between two transducers or between a transducer and a channel wall. By knowing the exact distance between the two transducers or the distance between the transducer and the reflective surface, one can calculate the sound velocity by dividing the distance by the acoustic pulse flight/delay time. The sound velocity in liquids is a function of the bulk modulus and bulk modulus changes with temperature. Therefore, by monitoring sound velocity, one can determine the average temperature of the liquid along the acoustic path.

On the other hand, ultrasonic heating is also well known. This method has been used for quite some time in physiotherapy for treating injuries, pain and inflammation. Focused acoustic beams are usually used for increased efficiency. In general, due to acoustic absorption inside the liquid where the ultrasound propagates, the temperature increases. In this paper, we will apply these two ultrasonic methods that have been used in macroscale to microfluidic channels.

## 2. Experimental

### 2.1. Channels with integrated piezoelectric transducers

Fig. 1 shows the fabricated microfluidic device with integrated piezoelectric transducers. The transducers have been formed by sandwiching a zinc oxide (ZnO) film between 1500 Å-thick gold electrodes on a quartz substrate. The ZnO film is deposited using the magnetron sputtering technique [25]. Electrodes are patterned using standard lithography steps. The transducers are  $300\ \mu\text{m} \times 300\ \mu\text{m}$ . The ZnO film thickness is  $8\ \mu\text{m}$ . On the other surface of the substrate, the channel is aligned to the transducers as shown in Fig. 2. The inlet and the outlet tubing are connected to the channel by means of holes drilled through the quartz substrate. The channel is made of glass and the width is  $500\ \mu\text{m}$ ; the height of the channel is approximately  $200\ \mu\text{m}$ . Fabrication details can be found in [5].

To test the transducers, the electrical input impedance has been measured by using a network analyzer. The first longitudinal res-

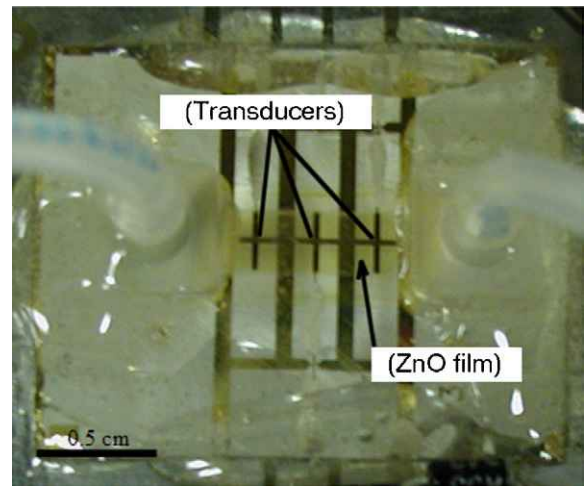


Fig. 1. Microfluidic channel with integrated transducers. Channel is on the bottom side of the substrate and is aligned to the transducers.

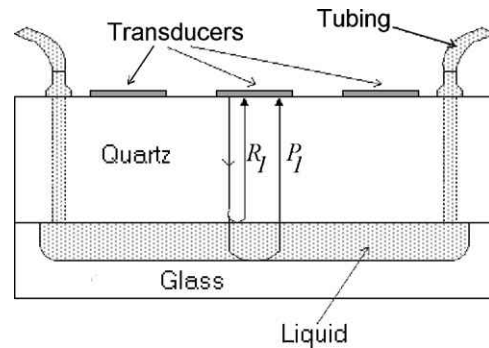


Fig. 2. Schematic of the devices showing the channel, transducers and tubing.

onance frequency of an  $8\ \mu\text{m}$ -thick ZnO film is approximately 400 MHz. However, due to the multiple resonances along the thickness of the quartz substrate, many resonance peaks are observed as shown in Fig. 3. The resonance peaks correspond to the multiple of the half wavelength of acoustic waves in quartz plate where the thickness is 1.27 mm. The sound velocity in quartz is 5613 m/s [26]; therefore, the separation between the peaks is 2.21 MHz.

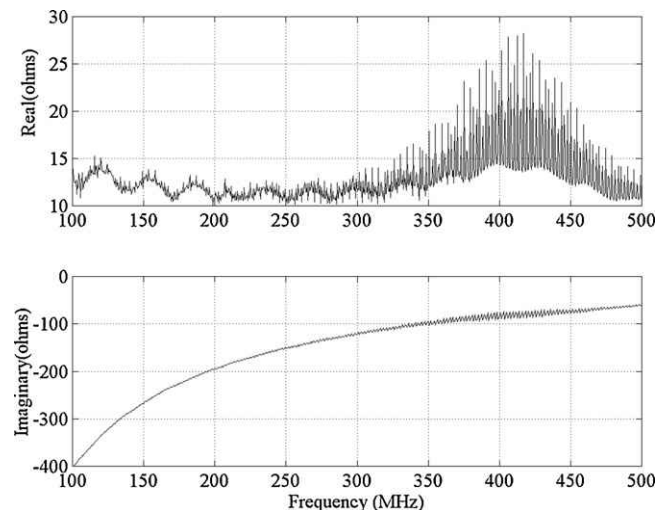


Fig. 3. Real (top) and imaginary (bottom) parts of the transducer impedance.

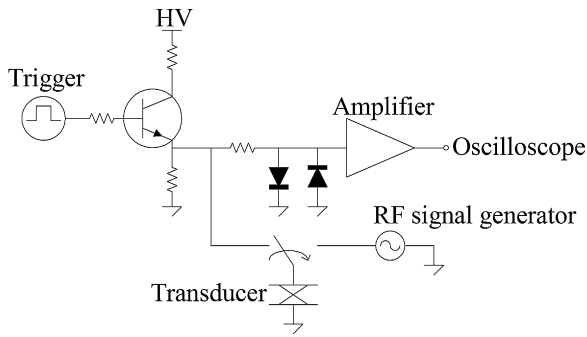


Fig. 4. Circuit used for pulse echo measurements and ultrasonic heating.

For pulse-echo measurements, we used the pulser circuit shown in Fig. 4. The main component of the circuit is a transistor, which is forced to operate in avalanche mode by a high bias voltage applied to its collector. Bias voltage ( $\sim 200$  V) has been obtained from a high voltage supply (SRS PS310, High voltage power supply). A trigger pulse, obtained from a function generator (Agilent 33250A, Function generator), is applied to the base of the transistor. When the pulse turns the transistor on, this allows charges accumulated in the transmission line to pass through the emitter of the transistor. This method enables the generation of the high-voltage, narrow-width pulses. The pulse width can be controlled by varying the length of the transmission line. In our experiments, we used 2-ns long 60 V pulses to drive ZnO transducers. The generated pulses are applied to the transducer where they are converted into longitudinal waves. In pulse echo mode, the relay connects the transducer to the emitter of the transistor. The acoustic pulses propagate in the substrate and then in the liquid filling the channel. After reflecting from the interfaces, they return back to the transducer where they are converted into electrical signals. Then, the received waveform passes through the protection circuitry and is amplified by microwave amplifiers. The protection circuit clips the amplitude of the high voltage pulse at the input of the amplifier such that the amplifier is not overloaded. For small amplitude pulses, the protection circuit works as a pass-through without affecting the amplitude. The received signal at the output of the amplifier is observed using an oscilloscope (HP Infiniium series). This circuit can also excite the transducer by a continuous sinusoidal voltage through a mechanical relay when the relay connects the signal generator to the transducer. The relay is controlled by another pulse generator to allow both heating and measurement modes. The ultrasonic measurement signal is recorded by an oscilloscope into a PC through GPIB connection for further analysis.

Fig. 5 shows the output voltage waveform of the amplifier. The first pulse, at approximately time zero, is the electrical feed through coupled from the transistor directly to the amplifier. This pulse is clipped by the protection diodes to prevent any damage to the amplifier. The second pulse, which is indicated by  $R_1$  in Fig. 5, is the reflection from the quartz-channel boundary. Other reflections ( $R_2, R_3, R_4, \dots$ ) are the multiples of this acoustic reflection. The separation of the pulses corresponds to the two-way time delay along the substrate thickness. When the channel is filled with a liquid, an additional reflection ( $P_1$ ) occurs between the first and second reflections as shown in Fig. 6. The time delay between the first reflection ( $R_1$ ) from the substrate-liquid interface (bottom of the channel) and the reflection ( $P_1$ ) from the liquid-glass interface (top of the channel) is given by

$$\Delta t = \frac{2h}{v} \quad (1)$$

where  $h$  is the channel height,  $v$  is the sound velocity inside the liquid. The liquid velocity and the attenuation change as a function

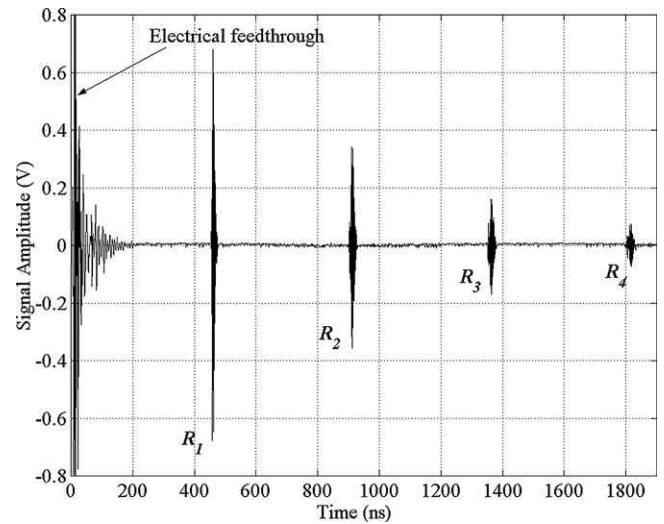


Fig. 5. Reflections inside the substrate.

of temperature. Fig. 7 shows the velocity and attenuation variation for DI water [26]. If the channel is filled with DI water, one can easily determine the temperature by measuring  $\Delta t$  and using the graph depicted in Fig. 7. However, instead of using Eq. (1), we used wave propagation calculations to improve the accuracy of the measurement. Due to the high acoustic attenuation in water in the vicinity of 400 MHz, the waves get dispersed after propagation in water. Therefore, different frequency components propagate with different amplitudes changing the initial pulse shape. In this case, it is difficult to set a threshold voltage on the received waveform for time delay measurements.

Accurate determination of temperature requires knowing the channel height precisely. This can be accomplished again by using the time of flight measurement. If a liquid with a known temperature fills the channel, one can find the channel height by using Eq. (1) or more accurately by using wave propagation calculations. We filled the channel with DI water and placed thermocouples inside the tubing as well as at different locations on the substrate to calibrate the channel height. DI water is well characterized in terms of acoustical properties [27,28]. We placed the whole system in a thermally isolated chamber and waited until all the thermocouples had shown the same temperature to make sure the water

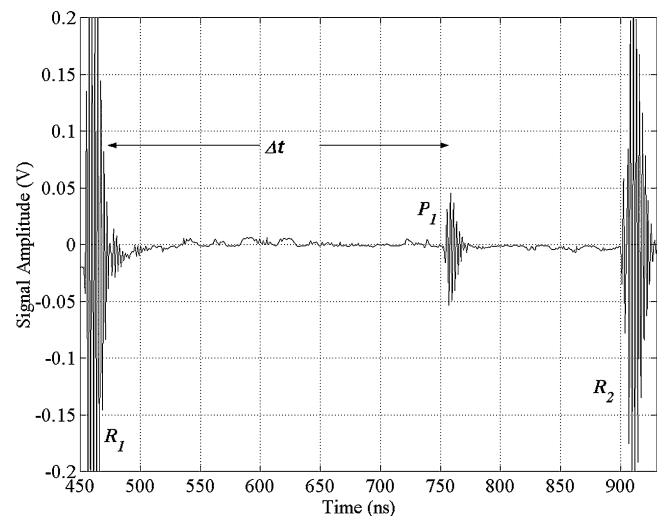


Fig. 6. Reflection from the channel top ( $P_1$ ) (zoomed version of Fig. 5 between  $R_1$  and  $R_2$  with the channel filled with DI water).

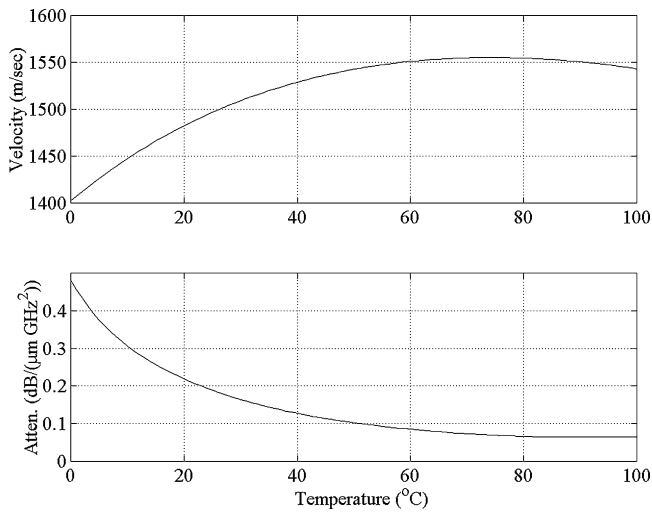


Fig. 7. Sound velocity and attenuation as a function of temperature for DI water.

temperature is the same throughout the channel. By using corresponding velocity to the measured temperature from Fig. 7 and time of flight measurement, we calculated the channel height. The resulting channel height is found to be 213.65  $\mu\text{m}$ .

### 3. Channels with integrated CMUTs

We also integrated channels with capacitive micromachined ultrasonic transducers (CMUTs). CMUTs have been developed for biomedical imaging in the frequency range of 1–5 MHz [29,30]. CMUTs can compete with piezoelectric transducers in terms of efficiency and bandwidth. Recently, it has been shown that CMUTs can be used for high frequency applications in the vicinity of 50 MHz [31]. This makes these transducers an attractive alternative for microfluidic applications since their manufacturing is IC fabrication compatible. This enables the integration of electronics and the microfluidic devices on the same silicon substrate.

Fig. 8 shows a microfluidic channel with integrated CMUTs. The CMUT is composed of many membranes, as shown in the zoomed picture of Fig. 8. Each membrane has a bottom electrode and a movable top electrode. When a sinusoidal voltage with a DC voltage is applied to the membranes, they vibrate due to the electrostatic forces between the electrodes and if an acoustic field impinges on a biased membrane, output current proportional to the field strength is generated. Fabrication steps for CMUT are described elsewhere [32]. For microfluidic applications, as the last fabrication step, an LPCVD oxide layer is deposited on top of the membranes to passivate the top electrode. Then, an SU-8 channel is aligned on top of the transducer. In contrast to the ZnO transducer, CMUTs can only be placed inside the channel, since they cannot couple ultrasound efficiently into the substrate.

The same circuit of Fig. 4 has been used for pulse-echo measurements. The operation frequency of this particular CMUT is approximately 40 MHz. Since the operation frequency is lower than that of ZnO film transducers, wider pulses have been used to excite the CMUTs. The pulse width is adjusted using a longer piece of transmission line. The obtained reflection waveform is depicted in Fig. 9. Since CMUTs send most of the energy into the immersion liquid, the waveform trace has only reflections from the channel top. The reflections from the liquid–glass interface are indicated by  $P_1$  and  $P_2$ . Other reflections, trailing  $P_1$  and  $P_2$ , are the multiple reflections inside the glass cover. The time of flight measurement requires the determination of the place of the  $P_1$  pulse.

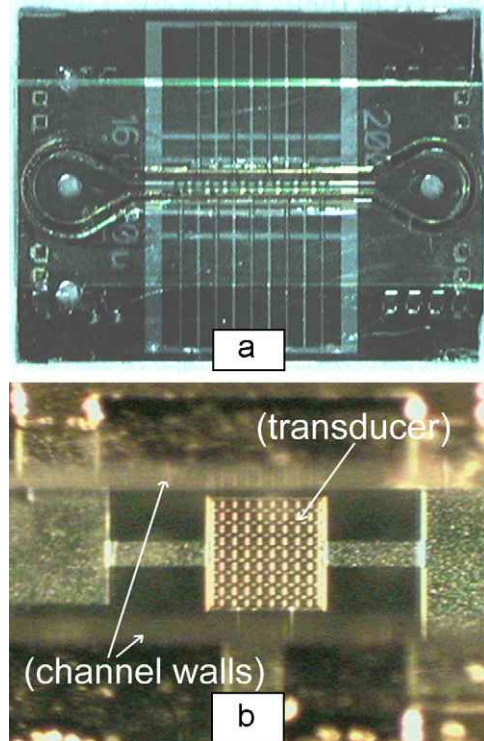


Fig. 8. (a) Microfluidic channel with integrated CMUTs; (b) zoomed on one transducer.

### 4. Results and discussion

We described two devices that we had used for temperature measurements. The piezoelectric transducer has both temperature measurement and heating capability with the help of the switch shown in Fig. 4. When the switch connects the RF generator to the transducer, the acoustic waves generated by the transducer increases the temperature of the liquid. The RF frequency is adjusted such that the transducer excites one of the thickness mode resonances of the substrate for improved efficiency. During measurement cycle, the switch connects the transistor to the transducer. In this case, the transistor was triggered by an off the shelf pulse generator. The obtained waveforms are shown in Fig. 10, schematically. The switch is driven by a square-wave of 10 Hz. The

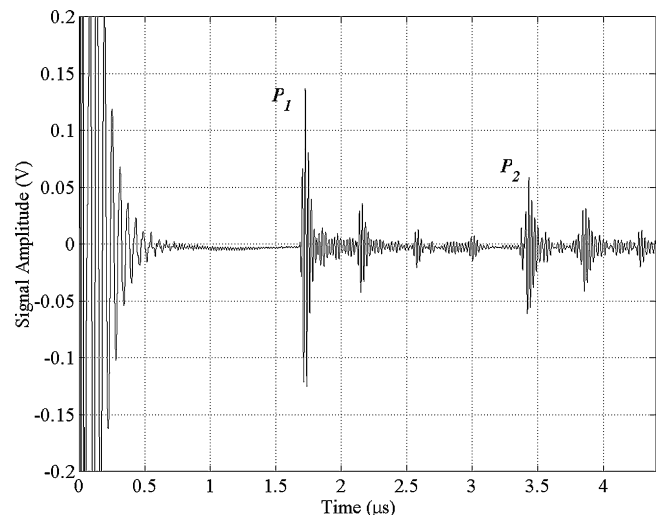


Fig. 9. Reflections inside the channel using CMUT.

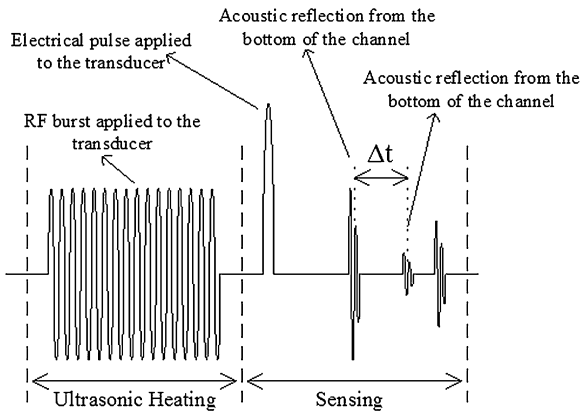


Fig. 10. Acoustic heating and sensing.

switch is also synchronized with the pulse generator that triggers the transistor. We chose 50% duty cycle for the 10 Hz square-wave that drives the switch. Thus, the liquid is heated for 50 ms followed by a measurement cycle. The time required for the temperature measurement was less than a microsecond. The only limitation on how soon one can measure the temperature after the heating cycle is that the multiple reflections inside the substrate have to decay completely prior to the temperature measurement. In the measurement cycle, the waveforms were stored in an oscilloscope memory and transferred to a computer by means of GP-IB interface.

Later, the stored waveforms are processed to find the temperature. The time of flight can be determined accurately by using a wave propagation calculation based algorithm. The reflection from the water–glass interface ( $P_1$ ) can be calculated by using the reflection ( $R_1$ ) from the substrate–liquid interface through the following equation:

$$P_1(t) = F^{-1} \{ F \{ R_1(t) \} e^{-jkz} \} L T_{QW} R_{WQ} T_{WQ} \quad (2)$$

where  $F\{\cdot\}$  and  $F^{-1}\{\cdot\}$  are Fourier and inverse Fourier transforms, respectively.  $t$  shows the time dependence.  $L$  indicates the attenuation in the liquid.  $T_{QW}$  is the transmission coefficient between the liquid and the quartz substrate whereas  $R_{WQ}$  is the reflection coefficient at the liquid and the glass interface. The phase due to the propagation in the liquid by distance  $z$  (channel height) is added through the exponential term and,

$$k = \frac{2\pi f}{v} \quad (3)$$

where  $f$  is the frequency. The above calculation involves the propagation of  $R_1$  pulse through the liquid filling the channel. First, one must assume a temperature for the liquid. By using the calibration curve, the velocity and the loss in the liquid are determined. The velocity and attenuation are later used to calculate the phase and the amplitude of the propagated pulse. For propagation calculation, first the Fourier transform of the pulse is calculated, and then the necessary phase is added due to the propagation inside the liquid. Reflection and transmission coefficients as well as the attenuation inside the liquid are also taken into consideration by modifying the pulse amplitude accordingly. Finally, calculating the inverse transform reveals the reflection from the top interface of the channel. This procedure is iterated on temperature until the best fit between the calculated pulse and the measured pulse is obtained. Fig. 11 shows the measured and calculated pulse when the best match was achieved for an arbitrarily chosen measurement. To increase the time resolution, we interpolated the measured waveform 8 times by padding zeros to the Fourier transform. In our measurements, typical time jitter on the measurements is around 0.05 ns. The

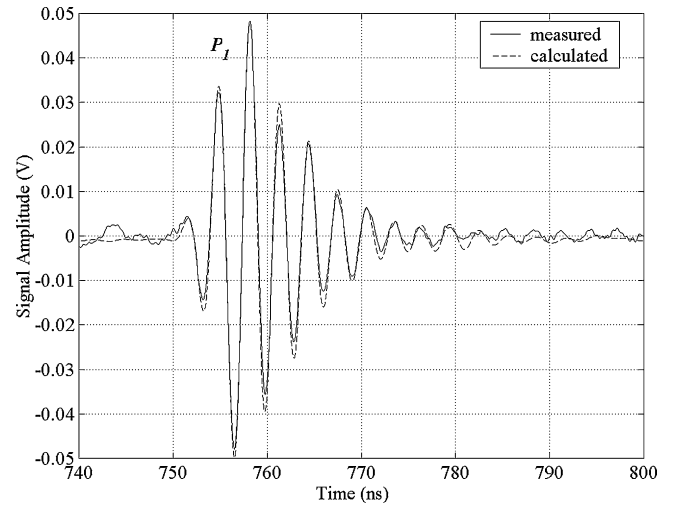


Fig. 11. Zoomed version of the water reflection. Measured and calculated.

corresponding temperature measurement error is approximately 0.1 °C.

The calculated temperature is shown in Fig. 12. The RF power was increased 5 dBm at every 2.5 min. The measurement demonstrates heating and measurement capability at the same time. The time constant observed on the graph depends on the duty cycle of the RF signal. For higher duty cycles one would expect faster heating. So far we have demonstrated non-real time measurement of temperature. However, one can directly measure the places of the pulses to find the time of flight by detecting zero crossings. The above algorithm improves the temperature accuracy when the amplitude of the reflection is small.

We repeated the temperature measurement experiment with CMUT devices. Instead of ultrasonic heating, an external source has been used in these experiments. The experimental setup is shown in Fig. 13. We removed the channel and replaced it by a glass plate supported by two spacers. The distance between the top surface of the silicon wafer and the bottom surface of the glass plate is approximately 1.2 mm. In this space, a thermocouple and a set of resistors are fitted as shown in Fig. 13. The resistor is used to heat the water filling the space. The channel height is calibrated using the thermocouple reading without applying any voltage to the heating resistor. Then, the voltage is increased by 0.5 V steps every 3 min. Fig. 14 compares the thermocouple reading and the ultrasonic method. For this measurement, only the change of the position of the maximum point of the pulse  $P_1$  is observed and the time of flight is converted into temperature using the curve in Fig. 4. For this mea-

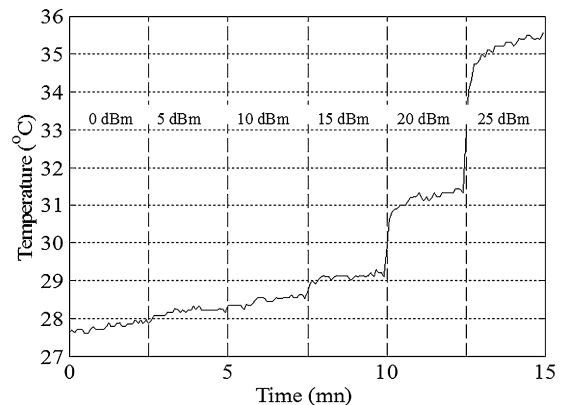


Fig. 12. Temperature measurement using ZnO (for both heating and measurement).

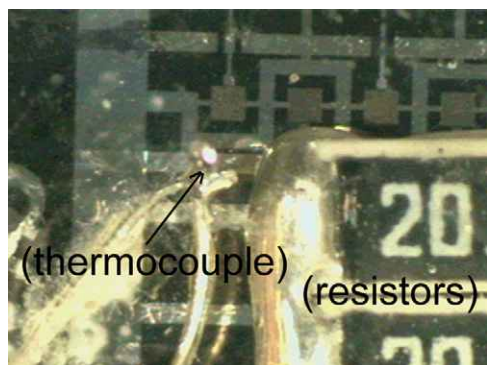


Fig. 13. Experimental setup for CMUT temperature measurement.

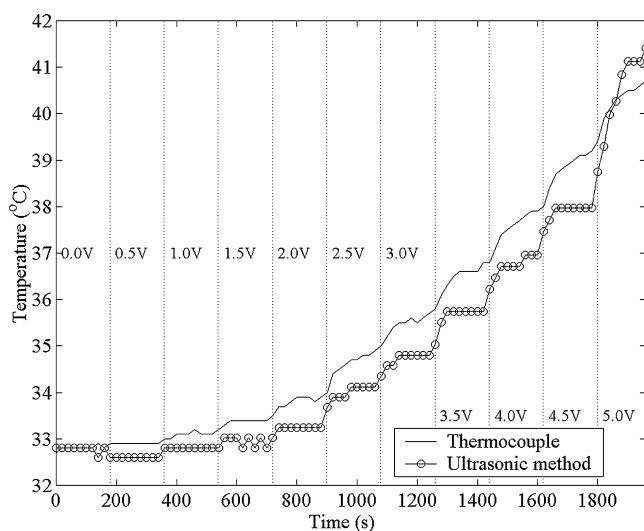


Fig. 14. Temperature measurement using CMUT.

surement the wave-propagation approach is not used due to the less dispersion at relatively lower frequency of 40 MHz.

## 5. Conclusions

We developed piezoelectric and CMUT based transducers and integrated them with the microfluidic channels for ultrasonic temperature measurements and heating. This method enables measurements with high bandwidth (1 MHz) and high accuracy (0.1 °C). The spatial resolution is determined by the transducer size and it measures the average temperature in the path of the ultrasonic waves. This method is insensitive to the temperature changes that occur on the substrate and it measures the absolute temperature of the liquid. We demonstrated two methods for temperature measurement: the wave propagation method and the direct method. The first method is not real-time and it uses wave propagation calculation. This method gives accurate results for high frequency transducers where dispersion due to the attenuation is high.

The ultrasonic temperature measurement method can also be applied when there is flow in the channel. The sound velocity in the channel is orders of magnitude higher than typical flow velocities. The effect of fluid flow on the time of flight is negligible.

One disadvantage of the ultrasonic measurement method is that one needs to know the relation between the sound velocity and the temperature to be able to convert velocity information to the temperature. This can be achieved by measuring the fluid velocity in a channel with known height using a well controlled temperature.

In this paper, we also achieved acoustic heating in microfluidic channels. Ultrasonic heating can be successfully applied in very small volumes where the temperature needs to be controlled accurately. The efficiency of the acoustic heating can be increased if a matching network is employed between the signal generator and the transducer.

Using the acoustic heating/measurement technique described in this paper, one can also implement flow measurement based on hot wire anemometer method. In this method, the flow inside the channel will determine the temperature rise for a given acoustical power. For high flow rates, the temperature increases less. Another flow measurement method is the Doppler shift detection. In this method, acoustic scattering is detected from the particles inside the fluid by a transducer. These may present themselves as the subject of future research topics.

## References

- [1] A. Manz, N. Graber, H.M. Widmer, Miniaturized total chemical analysis systems: a novel concept for chemical sensing, *Sens. Actuators B: Chem.* 1 (1990) 244–248.
- [2] P.S. Dittrich, K. Tachikawa, A. Manz, Micro total analysis systems: latest advancements and trends, *Anal. Chem.* 78 (2006) 3887–3908.
- [3] C.-M. Ho, Fluidics – the link between micro and nano sciences and technologies, in: *Proc. IEEE International Conference on MEMS*, 2001, pp. 375–384.
- [4] H. Andersson, A. van den Berg, Microfluidic devices for cellomics: a review, *Sens. Actuators B: Chem.* 92 (2003) 315–325.
- [5] G.G. Yaralioglu, I.O. Wygant, T.C. Marentis, B.T. Khuri-Yakub, Ultrasonic mixing in microfluidic channels using integrated transducers, *Anal. Chem.* 76 (2004) 3694–3698.
- [6] M.N. Slyadnev, Y. Tanaka, M. Tokeshi, Takehiko Kitamori, Photothermal temperature control of a chemical reaction on a microchip using an infrared diode laser, *Anal. Chem.* 73 (2001) 4037–4044.
- [7] D.J. Sadler, R. Changrani, P. Roberts, C.-F. Chou, F. Zenhausern, Thermal management of BioMEMS: temperature control for ceramic-based PCR and DNA detection devices, *IEEE Trans. Components Pack. Technol.* 26 (2003) 309–316.
- [8] D. Ross, M. Gaitan, L.E. Locascio, Temperature measurement in microfluidic systems using a temperature-dependent fluorescent dye, *Anal. Chem.* 73 (2001) 4117–4123.
- [9] V.N. Hoang, G.V. Kaigala, C.J. Backhouse, Dynamic temperature measurement in microfluidic devices using thermochromic liquid crystals, *Lab Chip* 8 (2008) 484–487.
- [10] A. Iles, R. Fortt, A.J. de Mello, Thermal optimisation of the Reimer–Tiemann reaction using thermochromic liquid crystals on a microfluidic reactor, *Lab Chip* 5 (2005) 540–544.
- [11] A.I.K. Lao, T.M.H. Lee, I.-M. Hsing, N.Y. Ip, Precise temperature control of microfluidic chamber for gas and liquid phase reactions, *Sens. Actuators A: Phys.* 84 (2000) 11–17.
- [12] C.H. Fan, J.P. Longtin, Laser-based measurement of liquid temperature or concentration at a solid–liquid interface, *Exp. Therm. Fluid Sci.* 23 (2000) 1–9.
- [13] L. Liu, S. Peng, W. Wen, P. Sheng, Micro thermoindicators and optical-electronic temperature control for microfluidic applications, *Appl. Phys. Lett.* 91 (2007) 093513.
- [14] K.T.V. Grattan, The use of fiber optic techniques for temperature measurements, *Meas. Control* 20 (1987) 32–39.
- [15] M.E. Lacey, A.G. Webb, J.V. Sweedler, Monitoring temperature changes in capillary electrophoresis with nanoliter-volume NMR thermometry, *Anal. Chem.* 72 (2000) 4991–4998.
- [16] K.L. Davis, K.L.K. Liu, M. Lanan, M.D. Morris, Spatially resolved temperature measurements in electrophoresis capillaries by Raman thermometry, *Anal. Chem.* 65 (1993) 293–298.
- [17] S.H. Kim, J. Noh, M.K. Jeon, K.W. Kim, L.P. Lee, S.I. Woo, Micro-Raman thermometry for measuring the temperature distribution inside the microchannel of a polymerase chain reaction chip, *J. Micromech. Microeng.* 16 (2006) 526–530.
- [18] K. Swinney, D.J. Bornhop, Non-invasive picoliter volume thermometry based on backscatter interferometry, *Electrophoresis* 22 (2001) 2032–2036.
- [19] G. Maltezos, M. Johnston, A. Scheren, Thermal management in microfluidics using micro-peltier junctions, *Appl. Phys. Lett.* 87 (2005) 154105.
- [20] M. Hashimoto, P.C. Chen, M.W. Mitchell, D.E. Nikitopoulos, S.A. Soper, M.C. Murphy, Rapid PCR in a continuous flow device, *Lab Chip* 4 (2004) 638–645.
- [21] A.J. de Mello, M. Habgood, N.L. Lancaster, T. Welton, R.C.R. Wootton, Precise temperature control in microfluidic devices using Joule heating of ionic liquids, *Lab Chip* 4 (2004) 417–419.
- [22] M. Mori, Y. Takeda, T. Taishi, N. Furuichi, M. Aritomi, H. Kikura, Development of a novel flow metering system using ultrasonic velocity profile measurement, *Exp. Fluids* 32 (2002) 153–160.
- [23] T. Vontz, V. Magori, A ultrasonic flow meter for industrial applications using a helical sound path, in: *Ultrasonics Symposium, Proceedings*, vol. 2, 1996, pp. 1047–1050.

- [24] P. Hauptmann, N. Hoppe, A. Püttmer, Application of ultrasonic sensors in the process industry, *Meas. Sci. Technol.* 13 (2002) R73–R83.
- [25] B.T. Khuri-Yakub, J.G. Smits, T. Barbee, Reactive magnetron sputtering of ZnO, *J. Appl. Phys.* 52 (1981) 4772–4774.
- [26] R.A. Lemons, C.F. Quate, Acoustic microscopy, in: W.P. Mason, R.N. Thurston (Eds.), *Physical Acoustics XIV*, Academic Press, London, 1979, pp. 1–92.
- [27] V.A. Del Grosso, C.W. Mader, Speed of sound in pure water, *J. Acoust. Soc. Am.* 52 (1972) 1442–1446.
- [28] W. Marczak, Water as a standard in the measurements of speed of sound in liquids, *J. Acoust. Soc. Am.* 102 (1997) 2776–2779.
- [29] H.T. Soh, I. Ladabaum, A. Atalar, C.F. Quate, B.T. Khuri-Yakub, Silicon micro-machined ultrasonic immersion transducers, *Appl. Phys. Lett.* 69 (1996) 3674–3676.
- [30] I. Ladabaum, X.C. Jin, H.T. Soh, A. Atalar, B.T. Khuri-Yakub, Surface micro-machined capacitive ultrasonic transducers, *IEEE Trans. Ultrason. Ferroelectr. Frequency Control* 45 (1998) 678–690.
- [31] A.S. Ergun, Y. Huang, C.H. Cheng, O. Oralkan, J.A. Johnson, H. Jagannathan, U. Demirci, G.G. Yaralioglu, M. Karaman, B.T. Khuri-Yakub, Broadband capacitive micromachined ultrasonic transducers ranging from 10 kHz to 60 MHz for imaging arrays and more, in: *Ultrasonics Symposium, Proceedings*, vol. 2, 2002, pp. 1039–1043.
- [32] A.S. Ergun, G.G. Yaralioglu, B.T. Khuri-Yakub, Capacitive micromachined ultrasonic transducers: theory and technology, *J. Aerospace Eng.* 16 (2003) 76–84.

## Biography

**Goksen G. Yaralioglu** received his B.S., M.S., and Ph.D. degrees from Bilkent University, Turkey, in 1992, 1994, and 1999, respectively, all in electrical engineering. He worked as an engineering research associate at E.L. Ginzton Laboratory, Stanford University between 1999 and 2006. His researches focused on MEMS transducers, microfluidics, ultrasonic imaging and atomic force microscopy. Currently, he is working at a start-up company where he is developing inertial sensors.